Monte-carlo and sensitivity transport model: application in solar energy

Zili HE, Paule Lapeyre, Stéphane Blanco, Simon Eibner, Mouna El-Hafi, Richard Fournier

MONTE-CARLO AND SENSITIVITY TRANSPORT MODEL: APPLICATION IN SOLAR ENERGY

Zili He,[1,*] Paule Lapeyre,[2] Stephane Blanco,[3] Simon Eibner,[1] Mouna El Hafi,[1] Richard Fournier[3]

[1] RAPSODEE - UMR CNRS 5302, Campus Jarlard, Albi, 81013, France
[2] Department of Mechanical and Mechatronics Engineering, University of Waterloo, Canada
[3] LAPLACE - UMR CNRS 5213, 118 Route de Narbonne, Toulouse, 31062, France

ABSTRACT. The classical transport model of radiative transfer uses the specific intensity as the descriptor. By differentiating the transport model of intensity with respect to a geometric parameter, a model of geometric sensitivity can be built. In this work, a classical model of intensity and models of geometric sensitivity are built with specular flat mirrors as the boundary conditions and are applied in a concentrated solar power plant. The sensitivities of the impacting power on the receiver with respect to the geometric parameters of each mirror are estimated by the Monte Carlo Method (MCM). Furthermore, by analyzing the sources in the models of geometric sensitivity, the contributions of the typical optical effects: spillage, blocking, and shadowing, to the sensitivity can also be estimated and analyzed, which is essential information to optimize the system.

1. INTRODUCTION

MCM is preferred for radiative transfer simulations involving complex geometries [1]. Motivated by the optimization processes, calculating the sensitivities (partial derivatives of an observable with respect to some parameters) has always been an open research problem in radiative transfer [2–6]. Recently, Lapeyre *et al.* [7] proposes to build a model of transport for the sensitivity of the intensity. The similitude of the transport of intensity and the sensitivity is studied.

Generally, the intensity $I \equiv I(\vec{x}, \vec{\omega}, \pi)$ is the descriptor of a radiative transfer system, which is a function of three independent variables: $\vec{x}$ the position vector, $\vec{\omega}$ the propagation direction, and $\ddot{\pi}$ a geometric parameter. In the medium, the transport of the intensity is described by the Radiative Transfer Equation (RTE) [8]. The RTE in an inhomogeneous cold medium has the following form, with κ_a the absorption coefficient, κ_s the scattering coefficient, and Φ the phase function:

$$\vec{\omega}\cdot\frac{\partial I(\vec{x},\vec{\omega},\ddot{\pi})}{\partial\vec{x}} = -\kappa_a(\vec{x})I(\vec{x},\vec{\omega},\ddot{\pi}) - \kappa_s(\vec{x})I(\vec{x},\vec{\omega},\ddot{\pi}) + \frac{1}{4\pi}\int_{\Omega'=4\pi}\kappa_s(\vec{x})I(\vec{x},\vec{\omega}',\ddot{\pi})\Phi(\vec{\omega}',\vec{\omega})d\vec{\omega}' \tag{1}$$

In the medium, the RTE of the sensitivity $s \equiv \partial_{\ddot{\pi}} I$ can be built by differentiating the RTE of intensity with respect to $\ddot{\pi}$. Since $\ddot{\pi}$ corresponds to the geometric parameters of mirrors, the radiative properties

of the medium do not depend on it. Therefore, the corresponding development is straightforward:

$$\vec{\omega} \cdot \frac{\partial s(\vec{x}, \vec{\omega}, \ddot{\pi})}{\partial \vec{x}} = -\kappa_a(\vec{x}) s(\vec{x}, \vec{\omega}, \ddot{\pi}) - \kappa_s(\vec{x}) s(\vec{x}, \vec{\omega}, \ddot{\pi}) + \frac{1}{4\pi} \int_{\Omega'=4\pi} \kappa_s(\vec{x}) s(\vec{x}, \vec{\omega}', \ddot{\pi}) \Phi(\vec{\omega}', \vec{\omega}) d\vec{\omega}' \tag{2}$$

The sensitivity is regarded as a physical quantity emitted, absorbed, scattered, and reflected in the system. We can then benefit from years of research in solving the transport problem of intensity (the radiative transfer equation) to solve the transport problem of sensitivity.

The radiative modeling involving specular flat mirrors is widely required in the research field of Concentrated Solar Power (CSP) [9][1], images synthesis [10][11] and optics [11]. The sensitivity of the observable with respect to the geometric parameters of the mirrors is important information but is hard to calculate. In this work, based on the study of Lapeyre *et al.* [12][7], we build the transport models of intensity and its sensitivities for a typical radiative system involving specular flat mirrors to determine the impacting power on the receiver and its sensitivities to the geometric parameters of each mirror. Furthermore, by identifying the sources in the model of sensitivity, the contributions of typical optical effects: spillage, blocking, and shadowing, to the sensitivities can also be calculated, and then a detailed sensitivity analysis can be performed for optimization purposes.

2. GENERAL MODELS

A typical radiative transfer system with specular flat mirrors and black-body surfaces is shown in Figure.1. We study a system that consists of specular flat mirrors $\mathscr{H}_i$, $\forall i \in \{1, 2, \ldots, n_{\mathscr{H}}\}$ and $n_{\mathscr{H}}$ is the total number of mirrors in the system, a receiver $\mathscr{R}$, the cold boundary $\mathscr{O}_l$ and the hot boundary $\mathscr{O}_s$. r, s, l, p, b indices refer to the receiver, the hot boundary, the cold boundary, the reflecting surface of mirrors, and the rearward surface of mirrors. $\vec{x}$ is the position vector, $\vec{\omega}$ the propagation direction, and $\ddot{\boldsymbol{\pi}} \equiv [\ddot{\pi}_{i,j}]$ the matrix of geometric parameters (Figure 1). j indexes the six geometric parameters of a mirror $\mathscr{H}_i$: $\ddot{\pi}_{i,1}$, $\ddot{\pi}_{i,2}$ and $\ddot{\pi}_{i,3}$ characterize the translations following the three axes in the global coordinate system $\vec{e}_1$, $\vec{e}_2$ and $\vec{e}_3$; $\ddot{\pi}_{i,4}$ and $\ddot{\pi}_{i,5}$ characterize the altazimuth mount according to the two vectors of rotation $\vec{a}_{i,\theta}$ and $\vec{a}_{i,\phi}$; $\ddot{\pi}_{i,6}$ characterizes the length of the square mirror. $\vec{x}$, $\vec{\omega}$, $\ddot{\boldsymbol{\pi}}$ are independent variables and matrix $\boldsymbol{s} \equiv [s_{i,j}(\vec{x}, \vec{\omega}, \ddot{\boldsymbol{\pi}})] = \partial_{\ddot{\boldsymbol{\pi}}} I(\vec{x}, \vec{\omega}, \ddot{\boldsymbol{\pi}})$ is defined as the matrix of sensitivity of the intensity [7].

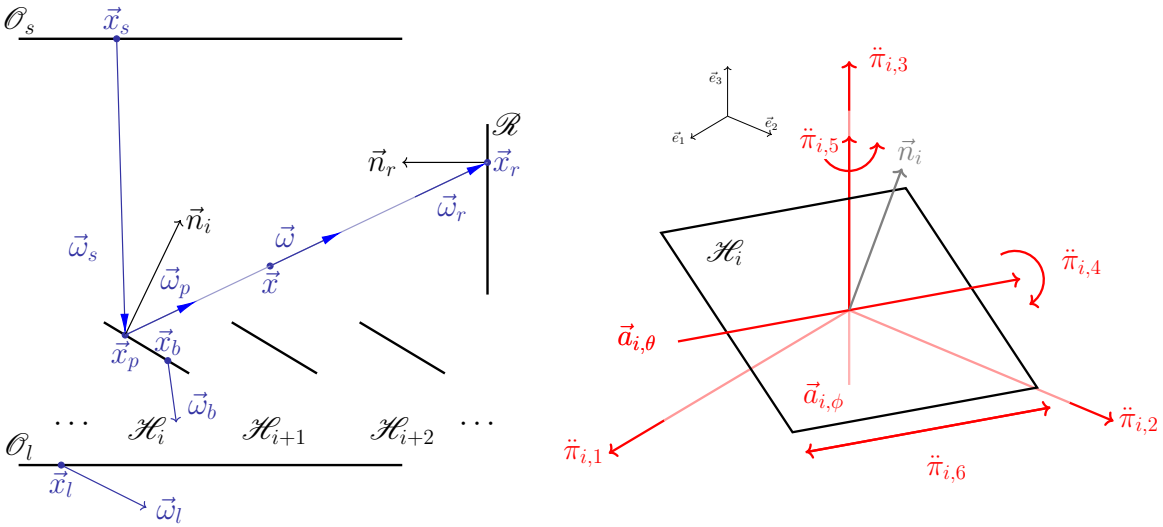

Figure 1. The radiative system (the left figure) and the studied parameters (the right figure). This figure is extracted from [13].

In this article, we study the sensitivity of the impacting power (Equation.5), with respect to the geometric parameters (Equation.6), in the context of solar power plants. Attenuation by absorption and scattering is often negligible. The first observation of P. Lapeyre (the intensity and the sensitivity propagations are identical in the medium, which can be seen by comparing Equation.1 and Equation.2) reduces to the following statement: As the intensity propagates along a straight line, the sensitivity also propagates along a straight line. The RTE for intensity and the sensitivity to a transparent medium leads to the following:

$$\frac{\partial I(\vec{x},\vec{\omega},\ddot{\boldsymbol{\pi}})}{\partial \vec{x}} = 0 \;\; ; \;\; \frac{\partial s_{i,j}(\vec{x},\vec{\omega},\ddot{\boldsymbol{\pi}})}{\partial \vec{x}} = 0 \tag{3}$$

However, the main question is modeling sensitivity on the boundaries and identifying the sensitivity sources. The PhD. thesis of P. Lapeyre focused on the formal mathematical development of the boundary conditions of the sensitivities, which is the tricky part of the model [14]. All the details of the model are available in [7].

2.1 Boundary conditions of the intensity

Before modeling the sensitivity on the boundaries, we must first model the intensity. The cold boundary, the receiver, and the rearward surfaces of the mirrors are considered cold black bodies. The reflecting surface of mirrors is considered cold and specular with the reflectivity ρ, and the source of intensity locates on the hot boundary within the solar cone.

$$\begin{cases} I(\vec{x}_r,\vec{\omega}_r) = 0;\; I(\vec{x}_l,\vec{\omega}_l) = 0;\; I(\vec{x}_b,\vec{\omega}_b) = 0 \;;\; I(\vec{x}_p,\vec{\omega}_p,\ddot{\boldsymbol{\pi}}) = \rho I(\vec{x},\vec{\omega}_s,\ddot{\boldsymbol{\pi}}) \\ I(\vec{x}_s,\vec{\omega}_s) \equiv \mathring{I}(\vec{\omega}_s) = I_0 \mathcal{H}(\vec{\omega}_s \cdot \vec{\omega}_c - \cos(\theta_{disk})) \end{cases} \tag{4}$$

where $\mathring{I}$ indicates the source of intensity. Herein, we model a source of intensity within a limited solid angle. It is a common assumption when considering the sun as the source of intensity in the system [15]. $\vec{\omega}_c$ is the vector that characterizes the solar position, I_0 the constant intensity from the sun, $\mathcal{H}$ the Heaviside function and $2 \times \theta_{disck} = 0{,}0093\,\mathrm{rad}$ the apparent diameter of the sun. In other words, the intensity coming from the solar cone around $\vec{\omega}_c$ is a constant. Otherwise, it is null.

2.2 Definitions of the observable and its sensitivities

The observable is the physical measure of the descriptor (the intensity) in the radiative system. It is usually the spatial or angular integral of the intensity. Herein, we take the impacting power of the receiver as an example. The impacting power is the sum of arriving intensities on the receiver:

$$P(\ddot{\boldsymbol{\pi}}) = \int_{\mathscr{R}} d\vec{x}_r \int_{2\pi} |\vec{\omega}_r \cdot \vec{n}_r| d\vec{\omega}_r I(\vec{x}_r,\vec{\omega}_r,\ddot{\boldsymbol{\pi}}). \tag{5}$$

The sensitivities of the observable $\boldsymbol{S}$ are its derivatives with respect to the parameters $\ddot{\boldsymbol{\pi}}$, which can be regarded as the sum of arriving sensitivities on the receiver:

$$\boldsymbol{S}(\ddot{\boldsymbol{\pi}}) \equiv \partial_{\ddot{\boldsymbol{\pi}}} P(\ddot{\boldsymbol{\pi}}) \equiv [S_{i,j}(\ddot{\boldsymbol{\pi}})] = \int_{\mathscr{R}} d\vec{x}_r \int_{2\pi} |\vec{\omega}_r \cdot \vec{n}_r| d\vec{\omega}_r \boldsymbol{s}(\vec{x}_r,\vec{\omega}_r,\ddot{\boldsymbol{\pi}}). \tag{6}$$

A transport model of I is already built. One can benefit from the work of [1] to build an efficient Monte Carlo algorithm to estimate $P(\ddot{\boldsymbol{\pi}})$. In order to estimate the matrix of sensitivities of the observable $\boldsymbol{S}$, transport models of the sensitivities $\boldsymbol{s}$ are needed.

2.3 Boundary conditions of the sensitivity and identification of sensitivity sources

Since the parameters $\ddot{\boldsymbol{\pi}}$ characterize only the mirrors, the boundary conditions of the cold boundary, the hot boundary, and the receiver do not depend on it:

$$s_{i,j}(\vec{x}_r, \vec{\omega}_r) = 0;\ s_{i,j}(\vec{x}_l, \vec{\omega}_l) = 0;\ s_{i,j}(\vec{x}_s, \vec{\omega}_s) = 0. \tag{7}$$

However, the development of the boundary conditions of $s_{i,j}$ for the mirror $\mathscr{H}_i$ is not that straightforward. Models of geometric sensitivity on reflecting surfaces and an opaque surface are proposed by [7]. Based on these two models, the boundary conditions of the reflecting surface and the rearward surface of the mirror are described. The reflecting surface consists of emission terms, as known as the sources of the sensitivity, and a reflection term (Equation 8). The rearward surface consists of emission terms (Equation 9).

$$s_{i,j}(\vec{x}_p, \vec{\omega}_p, \ddot{\boldsymbol{\pi}}) = \mathring{s}_{i,j}(\vec{x}_p, \vec{\omega}_p, \ddot{\boldsymbol{\pi}}) + \rho s_{i,j}(\vec{x}_p, \vec{\omega}_s, \ddot{\boldsymbol{\pi}}) \tag{8}$$

$$s_{i,j}(\vec{x}_b, \vec{\omega}_b, \ddot{\boldsymbol{\pi}}) = \mathring{s}_{i,j}(\vec{x}_b, \vec{\omega}_b, \ddot{\boldsymbol{\pi}}) \tag{9}$$

$\mathring{s}_{i,j}$ is noted as the source of $s_{i,j}$ (as we noted $\mathring{I}$ as the source of I). The source $\mathring{s}_{i,j}$ can be physically regarded as the local perturbations of I with respect to $\ddot{\pi}_{i,j}$. For example, in the left figure of the Figure. 2, the intensity (in blue color) arrives on the mirror. The perturbation of the parameter $\ddot{\pi}_{i,1}$ causes the perturbations of reflected intensity. These perturbations are regarded as the sources of sensitivities and are drawn in red color. The other term on the right side of Equation 8 represents the reflection of such perturbation. Moreover, different types of perturbation (sources) are distinguished in this work, related to different optical effects.

On the reflecting surface of $\mathscr{H}_i$:

$$\mathring{s}_{i,j}(\vec{x}_p, \vec{\omega}_p, \ddot{\boldsymbol{\pi}}) = \mathring{s}^{tar}_{i,j}(\vec{x}_p, \vec{\omega}_p, \ddot{\boldsymbol{\pi}}) + \mathring{s}^{blo}_{i,j}(\vec{x}_p, \vec{\omega}_p, \ddot{\boldsymbol{\pi}}) + \mathring{s}^{shad-b}_{i,j}(\vec{x}_p, \vec{\omega}_p, \ddot{\boldsymbol{\pi}}) \tag{10}$$

and on the rearward surface of $\mathscr{H}_i$:

$$\mathring{s}_{i,j}(\vec{x}_b, \vec{\omega}_b, \ddot{\boldsymbol{\pi}}) = \mathring{s}^{shad-f}_{i,j}(\vec{x}_b, \vec{\omega}_b, \ddot{\boldsymbol{\pi}}). \tag{11}$$

$\mathring{s}^{tar}_{i,j}$, $\mathring{s}^{blo}_{i,j}$, $\mathring{s}^{shad-b}_{i,j}$ and $\mathring{s}^{shad-f}_{i,j}$ are called the source of targeting, backward-blocking, backward-shadowing, and forward-shadowing respectively. Their physical illustration will be done by two specific configurations, and their explicit mathematical expression can be found in [7,13].

Configuration with only one mirror When we focus on only one mirror, the perturbation of $\ddot{\boldsymbol{\pi}}$ is related to the "targeting effect" (Figure 2). It consists of two kinds of perturbation: spatial perturbation and angular perturbation. For example, the perturbation of $\ddot{\pi}_{i,1}$ causes the change of mirror position, leading to the perturbation of intensity on its border (figure on the left). This perturbation of intensity is noted as the corresponding source of sensitivity $\mathring{s}^{tar,spatial}_{i,1}$. The perturbation of $\ddot{\pi}_{i,4}$ causes the change of position and also the change of normal, leading to the perturbation of intensity on the solar cone border (figure on the right). This perturbation is noted as $\mathring{s}^{tar,angular}_{i,4}$. Therefore, the corresponding source of sensitivity has two parts:

$$\mathring{s}^{tar}_{i,j} = \mathring{s}^{tar,spatial}_{i,j} + \mathring{s}^{tar,angular}_{i,j}. \tag{12}$$

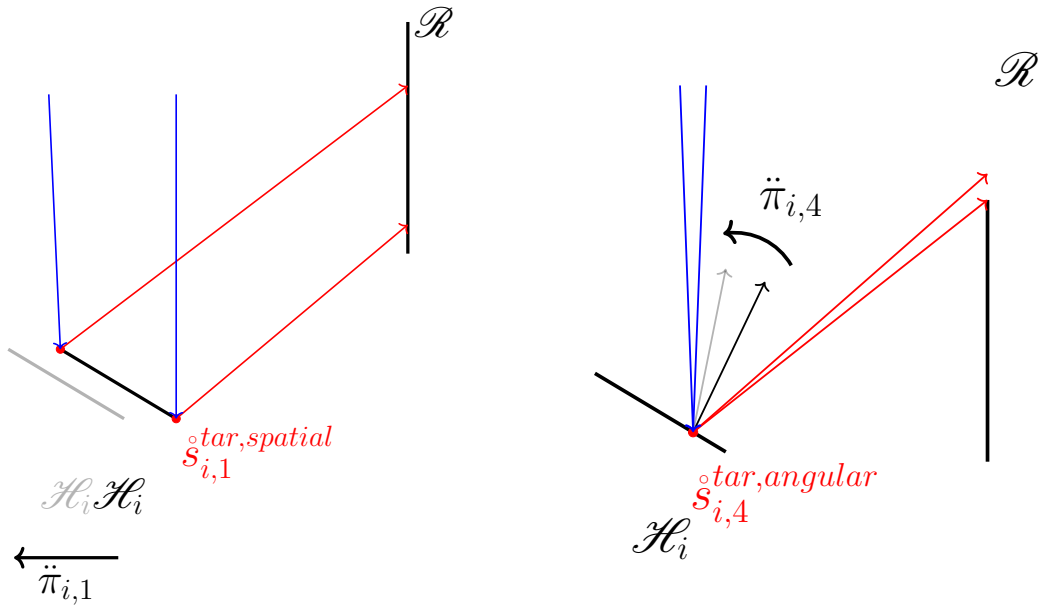

Figure 2. The perturbation of $\ddot{\pi}_{i,1}$ leads to two targeting perturbations of the intensity: the spatial one and the angular one. This figure is extracted from [13].

Configuration with four mirrors A perturbation on the geometric parameters $\ddot{\boldsymbol{\pi}}$ also interacts with the neighboring mirrors. For example, in Figure 3, besides the targeting effect, the perturbation of $\ddot{\boldsymbol{\pi}}$ is also related to the backward-blocking effect, backward-shadowing effect, and forward-shadowing effect. Two examples are shown here. The perturbation of $\ddot{\pi}_{i,1}$ blocks or unblocks the optical path passing through the border of $\mathscr{H}_i$, coming from the reflection on $\mathscr{H}_{i'}$. The source of sensitivity $\mathring{s}^{blo}_{i,1}$ is then located on the border of $\mathscr{H}_i$. Also, the perturbation impacts the shadow on $\mathscr{H}_{i'''}$, created by $\mathscr{H}_i$ itself. $\mathring{s}^{shad-f}$ is then located on the border of $\mathscr{H}_i$. Finally, the perturbation also impacts the shadow on $\mathscr{H}_i$ itself. The source $\mathring{s}^{shad-b,spatial}_{i,1}$ characterises the change of position and $\mathring{s}^{shad-b,angular}$ characterises the change of normal. Similar to the targeting effect, the source of backward-shadowing has two parts:

$$\mathring{s}^{shad-b}_{i,j} = \mathring{s}^{shad-b,spatial}_{i,j} + \mathring{s}^{shad-b,angular}_{i,j}. \tag{13}$$

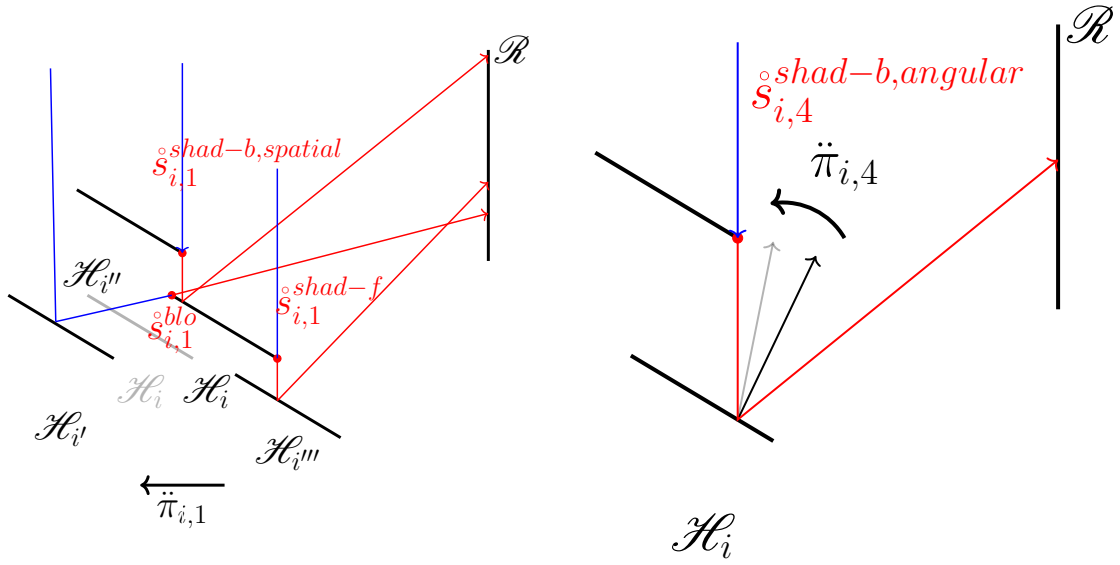

Figure 3. The perturbation of $\ddot{\pi}_{i,1}$ leads to the perturbations of shadowing and blocking. This figure is extracted from [13].

2.4 Calculating the sensitivity of the observable and its contributions

The model of $s_{i,j}$ is built at this stage. We note $S_{i,j}^{tar}$, $S_{i,j}^{blo}$, $S_{i,j}^{shad-b}$ and $S_{i,j}^{shad-f}$ as the sum of corresponding sources impacting the receiver. Physically, they are different kinds of perturbation of the intensity captured by the receiver:

$$\begin{bmatrix} S_{i,j}^{tar}(\ddot{\boldsymbol{\pi}}) \\ S_{i,j}^{blo}(\ddot{\boldsymbol{\pi}}) \\ S_{i,j}^{shad-b}(\ddot{\boldsymbol{\pi}}) \\ S_{i,j}^{shad-f}(\ddot{\boldsymbol{\pi}}) \end{bmatrix} = \int_{\mathscr{R}} d\vec{x}_r \int_{2\pi} |\vec{\omega}_r \cdot \vec{n}_r| d\vec{\omega}_r \begin{bmatrix} \mathring{s}_{i,j}^{tar}(\vec{x}_r, \vec{\omega}_r, \ddot{\boldsymbol{\pi}}) \\ \mathring{s}_{i,j}^{blo}(\vec{x}_r, \vec{\omega}_r, \ddot{\boldsymbol{\pi}}) \\ \mathring{s}_{i,j}^{shad-b}(\vec{x}_r, \vec{\omega}_r, \ddot{\boldsymbol{\pi}}) \\ \mathring{s}_{i,j}^{shad-f}(\vec{x}_r, \vec{\omega}_r, \ddot{\boldsymbol{\pi}}) \end{bmatrix}. \tag{14}$$

The sensitivity of the observable $S_{i,j}$ is the sum of all contributions. Physically, it is the sum of all kinds of perturbation captured by the receiver:

$$S_{i,j} = S_{i,j}^{tar} + S_{i,j}^{blo} + S_{i,j}^{shad-b} + S_{i,j}^{shad-f} \tag{15}$$

3. RESULTS

The developed method is then applied to a functioning solar power station: Sierra SunTower [16]. We addressed our calculation to a quarter of the mirror field for symmetry considerations. For each mirror in the field, the sensitivities of impacting power with respect to the six parameters (shown in Figure 1) are calculated. Only the results of $[S_{i,1}]$ and $[S_{i,6}]$ are shown here (Figure 4) because of the given space constraint. Each point represents a mirror, and the receiver is located at (0,0) at 50 meters high. The sun is at the position of local solar noon at the summer solstice, and the y-axis points to the south. The corresponding color indicates its sensitivity. It is observed that some mirrors at different locations are more sensitive than others. For example, the sensitivities of the left column on the left figure of Figure.4 are negative because the perturbation due to the translation following the positive x-axis direction makes them hidden behind the neighboring mirrors.

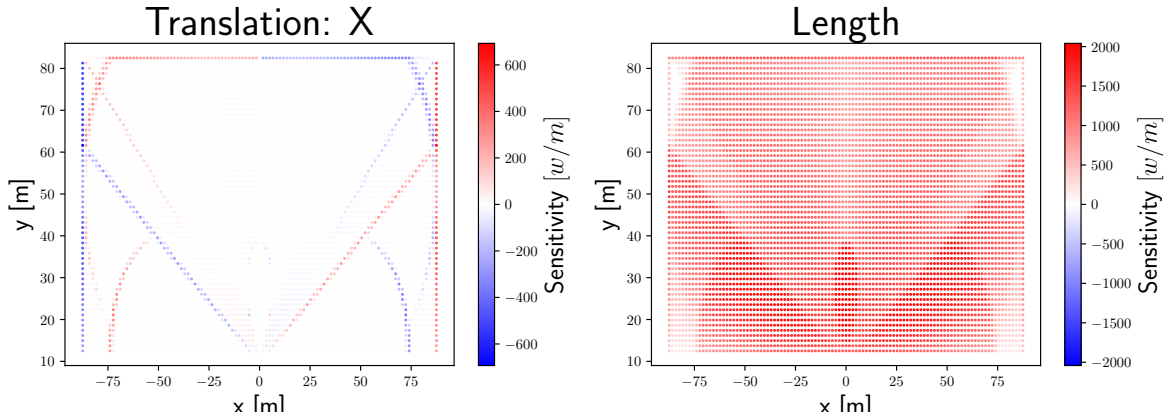

Figure 4. Sensitivities of the impacting power with respect to the translation following the x-axis (left figure) and the length of mirrors (right figure). This figure is extracted from [13].

Moreover, a comparison of results obtained by our method and the finite difference method is performed (see Table.1). Following the finite difference method, the sensitivity of the size of the 5297^{th} mirror is approximated by the two Monte Carlo estimations of the power: $\tilde{S} = \frac{P(\ddot{\pi}+\Delta\ddot{\pi}) - P(\ddot{\pi}-\Delta\ddot{\pi})}{2\Delta\ddot{\pi}}$. The corresponding standard deviation is also approximated [17]:$\sigma(\tilde{S}) \approx \frac{\sigma(P(\ddot{\pi}+\Delta\ddot{\pi})) + \sigma(P(\ddot{\pi}-\Delta\ddot{\pi}))}{2\Delta\ddot{\pi}}$. The result of the finite difference which takes a long calculation time, is still not reliable because of the heigh standard deviation compared to the approximated value. However, our method (MCM) converges almost instantaneously. According to the correlation between the Monte Carlo computation

time and the precision [17], the finite difference method will take 2×10^{11} more time of computation time to have the same accuracy of our method. Also, it is noted that the calculations are run on an ordinary laptop (4 CPUs of i5 Intel™, 8th generation).

Table 1: Estimated result of the sensitivity of the size (indexed as 6) of the 5297^{th} mirror by our method (MCM), compared and validated by the approximation of the finite difference method.

Finite difference method	Value	standard deviation	calculation time
$P(\ddot{\pi}_{5297,6} - \Delta\ddot{\pi}_{5297,6})$	$3231.62[w]$	$0.0389[w]$	$272.5[s]$
$P(\ddot{\pi}_{5297,6} + \Delta\ddot{\pi}_{5297,6})$	$3231.85[w]$	$0.0389[w]$	$272.5[s]$
$\tilde{S}_{5297,6}(\ddot{\pi}_{5297,6})$	$1.15[w/m]$	$0.389[w/m]$	$545[s]$
Our method (MCM)	Value	standard deviation	calculation time
$S_{5297,6}(\ddot{\pi}_{5297,6})$	$1.14974[w/m]$	$0.000041[w/m]$	$0.188[s]$

Last but not least, not only the sensitivities but also the contributions of sensitivities are estimated. Table 2 shows the sensitivity of the translation following the positive x-axis direction of the 676^{th} mirror. A perturbation of this translation will make the mirror less blocked by the one in front of it (the contribution $S^{tar}_{676,1}$ is positive). However, the mirror behind will be blocked more (the contribution $S^{blo}_{676,1}$ is negative) and see Figure 5. The total sensitivity is then the sum of these two contributions. Similarly, each sensitivity estimated by our method is the sum of its contributions so that a detailed physical analysis of sensitivity is possible.

Table 2: Sensitivity and its contributions (estimated values and their standard deviations) for the translation X of the 676^{th} mirror.

unit	$\mathrm{W\,m^{-1}}$
$S^{tar}_{676,1}$	70.63 ± 0.94
$S^{blo}_{676,1}$	-30.69 ± 0.58
$S_{676,1}$	39.93 ± 1.51

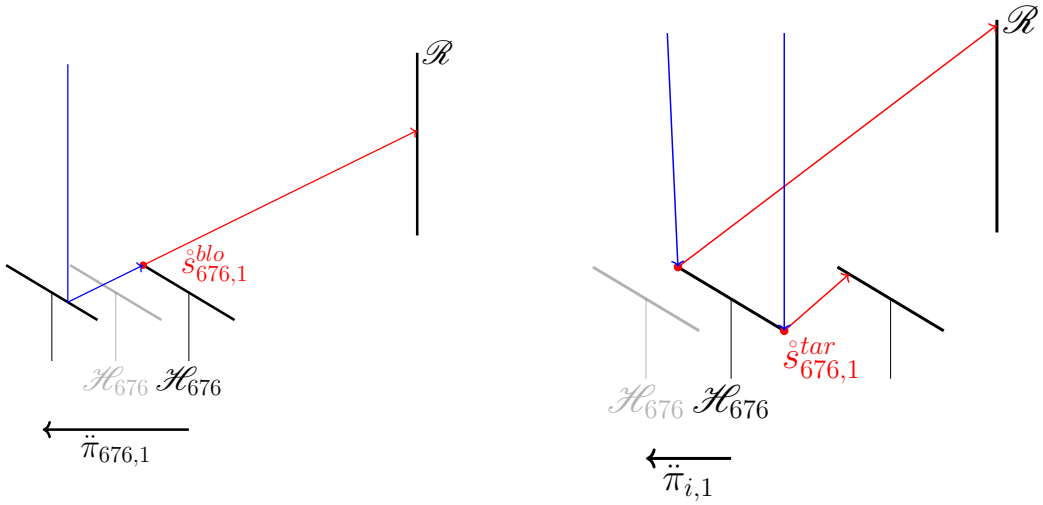

Figure 5. Two contributions of $S_{674,1}$: a positive contribution from the targeting effect and a negative contribution from the backward-blocking effect. This figure is extracted from [13].

4. CONCLUSION

A radiative transfer model is built for solar power plants using the intensity I as the descriptor. By differentiating the model of intensity, models of the sensitivity of the intensity with respect to different parameters $s_{i,j}$ are built. The observable, impacting power on the receiver and its sensitivities with

respect to the geometric parameters of the mirrors can be estimated by the MCM [1]. Moreover, this method allows us to distinguish sensitivity sources related to the targeting, backward-blocking, backward-shadowing, and forward-shadowing effects, which allows us to estimate contribution by contribution for each sensitivity and perform a detailed optimization process. Finally, the geometric sensitivities and their physical contributions can be estimated and analyzed in detail in a solar power plant. From the results of this work, engineers and researchers can couple our method with a gradient-based optimization algorithm to optimize a CSP system and perform a detailed sensitivity analysis.

ACKNOWLEDGMENTS

We thank the Region Occitanie, IMT Mines-Albi for the financial support of this research and the Labex SOLSTICE (ANR-10-LABX-22-01).

REFERENCES

[1] J. Delatorre, G. Baud, J.-J. Bézian, S. Blanco, C. Caliot, J.-F. Cornet, C. Coustet, J. Dauchet, M. El Hafi, V. Eymet, *et al.*, "Monte Carlo advances and concentrated solar applications," *Solar Energy*, vol. 103, pp. 653–681, 2014.

[2] E. Gobet, "Stochastic differential equations and Feynman-Kac formulas," in *Monte-Carlo Methods and Stochastic Processes*, Chapman and Hall/CRC, 2016. Num Pages: 46.

[3] A. J. Marston, "Geometric Optimization Of Solar Concentrating Collectors Using Quasi-Monte Carlo Simulation," M.Sc. Thesis, University of Waterloo, 2010.

[4] A. Marston, K. Daun, and M. Collins, "Geometric optimization of concentrating solar collectors using monte carlo simulation," *Journal of solar energy engineering*, vol. 132, no. 4, 2010.

[5] A. De Lataillade, S. Blanco, Y. Clergent, J.-L. Dufresne, M. El Hafi, and R. Fournier, "Monte Carlo method and sensitivity estimations," *Journal of Quantitative Spectroscopy and Radiative Transfer*, vol. 75, no. 5, pp. 529–538, 2002.

[6] M. Roger, S. Blanco, M. El Hafi, and R. Fournier, "Monte Carlo estimates of domain-deformation sensitivities," *Physical review letters*, vol. 95, no. 18, p. 180601, 2005.

[7] P. Lapeyre, Z. He, S. Blanco, C. Caliot, C. Coustet, J. Dauchet, M. E. Hafi, S. Eibner, E. d'Eon, O. Farges, R. Fournier, J. Gautrais, N. C. Mourtaday, and M. Roger, "A physical model and a Monte Carlo estimate for the specific intensity spatial derivative, angular derivative and geometric sensitivity," *arXiv*, 2022.

[8] J. R. Howell, M. P. Mengüç, K. Daun, and R. Siegel, *Thermal radiation heat transfer*, CRC press, 2020.

[9] C. K. Ho, "Advances in central receivers for concentrating solar applications," *Solar energy*, vol. 152, pp. 38–56, 2017.

[10] M. Kurt and D. Edwards, "A Survey of BRDF Models for Computer Graphics," *SIGGRAPH Comput. Graph.*, vol. 43, may, 2009.

[11] R. Montes and C. Ureña, "An overview of BRDF models," *University of Grenada, Technical Report LSI-2012-001*, 2012.

[12] P. Lapeyre, S. Blanco, C. Caliot, J. Dauchet, M. El Hafi, R. Fournier, O. Farges, J. Gautrais, and M. Roger, "Monte-Carlo and sensitivity transport models for domain deformation," *Journal of Quantitative Spectroscopy and Radiative Transfer*, vol. 251, p. 107022, 2020.

[13] Z. He, P. Lapeyre, S. Blanco, S. Eibner, M. El Hafi, and R. Fournier, "Monte-Carlo estimation of geometric sensitivities in Solar Power Tower systems of flat mirrors," *Solar Energy*, vol. 253, pp. 9–29, 2023.

[14] P. Lapeyre, "Un modèle de transfert radiatif pour la sensibilité géométrique: lecture physique des algorithmiques de Monte-Carlo via la double randomisation," PhD thesis, Perpignan, 2021.

[15] Y. Wang, D. Potter, C.-A. Asselineau, C. Corsi, M. Wagner, C. Caliot, B. Piaud, M. Blanco, J.-S. Kim, and J. Pye, "Verification of optical modelling of sunshape and surface slope error for concentrating solar power systems," *Solar Energy*, vol. 195, pp. 461–474, 2020.

[16] S. Schell, "Design and evaluation of esolar's heliostat fields," *Solar Energy*, vol. 85, no. 4, pp. 614–619, 2011.

[17] W. L. Dunn and J. K. Shultis, *Exploring monte carlo methods*, Elsevier, 2011.